Discrete Multi-Tone and Filtered Multi-Tone Architectures for Broadband Asynchronous Multi-User Communications

Andrea M. Tonello, and Silvano Pupolin

University of Padova – DEI - Department of Electronics and Informatics
Via Gradenigo 6/A, 35131 Padova, Italy
tonello@dei.unipd.it, pupolin@dei.unipd.it

Abstract

Multi-carrier systems based on both discrete multi-tone and filtered multi-tone architectures are investigated for application to asynchronous multi-user communications. Multiplexing of users is implemented by assigning a sub-set of the available carriers to each user. Communications are asynchronous, meaning that the signals belonging to distinct users propagate through independent frequency selective fading channels, and experience time and frequency misalignments due to propagation delays and movements (e.g., uplink communications). In this scenario inter-symbol, inter-carrier, and multiple access interference arise. We study the effect of the shape of the filters, as well as of the tones allocation strategy, on the interference components. We devise design guidelines for robust asynchronous multiple access communications based on multi-carrier architectures. Finally, we report performance results from simulations for several uncoded and coded systems.

Key words

Multi-carrier systems, multi-user communications, OFDM.

1. Introduction

This paper deals with multicarrier modulation for asynchronous multiple access broadband wireless communications. Each user deploys multicarrier modulation and accesses the media in a frequency division mode, FDMA. A given user is assigned a sub-set of the available carriers that are used to modulate parallel streams of information. We consider a particular form of multi-carrier modulation, where carriers are spaced by the inverse of the transmission symbol period, referred to as orthogonal frequency division multiplexing, OFDM. Each information stream is first filtered with an appropriate filter (referred to as prototype filter) and then carrier modulated. In general, the filters are not limited in time and in frequency, such that the scheme is referred to as filtered multi-tone multiple access, FMT-MA. A tutorial presentation of FMT modulation can be found in [1]. When the filters are rectangular pulses then the scheme is commonly referred to as discrete multi-tone multiple access, DMT-MA. Some investigation of DMT-MA has been done in [2]. More general results can be found in [3]-[5].

In both architectures high spectral efficiency is achieved since a large number of sub-carriers with overlapping spectra is used. The deployment of different prototype filters, and tone allocation strategies, results in different multiple access architectures. All can be efficiently implemented with banks of poly-phase filters and Fast Fourier Transforms.

We address the impact of the prototype filter shape and the tone allocation method on the interference components that arise in an asynchronous scenario, e.g., uplink communications.

It is well known that the schemes based on OFDM are very sensitive to the time and frequency offsets. For this reason most of the work on OFDM has been done for synchronous downlink communications [6]. In the uplink, the signals transmitted by users at different distances from the base station are received with different time delays. The presence of multi-path fading introduces echoes, such that the received signal is the superposition of multiple replicas of the signals transmitted by all users. Furthermore, a frequency offset is present among users whenever their local oscillators are misadjusted and/or movements introduce a frequency Doppler shift.

We show through analysis that, in this scenario, inter-symbol (ISI), inter-carrier (ICI), and multiple access interference (MAI) components arise at the output of the receiver sub-channel matched filters. The interference components are a function of the prototype filters, the tone allocation strategy, and the propagation conditions, i.e., channel time/frequency characteristics and time/frequency offsets.

To minimize the interference components, it is found that practically time and frequency limited filters are required. For instance, a good choice is to deploy Gaussian shaped filters.

This paper is organized as follows. In Section 2 we describe the transmitter architecture. In Section 3 we describe the asynchronous channel model. Section 4 deals with the receiver front-end. In section 5 we evaluate the interference components for several filter options. Design guidelines are devised in Section 6. Performance results are shown in Section 7 for several uncoded and coded systems. Finally, the conclusions follow.

2. Transmitter Model

2.1. Multiplexing of Users

Let $W=1/T$ be the total available bandwidth. This is divided into N equally spaced carriers $\bar{f}_k = \bar{f}_c + f_k$ with $f_k = k/(NT)$. Each user is assigned a subset of such carriers according to a given tone allocation strategy.

A number of carrier allocation methods are possible [4]. For instance, the spectrum can be partitioned into a number of blocks of carriers. A given block is assigned to a given user. We refer to it as block allocation. Another strategy is to

Part of this work was supported by MURST "PRIN 2000".
A. Tonello is on leave from Lucent Technologies – Bell Labs, Whippany, NJ USA.

ISBN: 87-988568-0-4

interleave the carriers across users, and we refer to it as interleaved allocation.

It follows that the system is a frequency division multiple access multi-carrier system.

2.2. Multi-carrier Modulation

A filter bank implementation of the transmitter of user u is shown in Fig. 1. The sequence of information bits belonging to user u, is mapped into a sequence of complex M-PSK/M-QAM symbols $\{x^u(nT)\}$. This sequence is S/P converted and formatted into N sub-sequences $\{x^{u,k}(lNT)\}$, $k=0,...,N-1$. If K_u is the number of carriers assigned to user u, then K_u out of N sub-sequences differ from zero.

The data sequences are sent through a polyphase filter bank. The impulse response of the *k-th* filter of user u is

$$g_T^{u,k}(t) = g_1^{u,k}(t)e^{j2\pi f_{u,k}t} \tag{1}$$

with $f_{u,k} = k/(NT)$ for a given index $k=0,...,N-1$.

The filter bank outputs are summed together. Thus, the complex multicarrier signal transmitted by user u, before RF modulation, is[1]

$$X^u(t) = \sum_{k=0}^{N-1}\sum_{l=-\infty}^{\infty} x^{u,k}(lNT)g_T^{u,k}(t-lNT) \tag{2}$$

The prototype filters $g_1^{u,k}(t)$ are designed with the goal of minimizing the inter-carrier (ICI), inter-symbol (ISI), and multiple access (MAI) interference. In general they are not limited in time and frequency, therefore the system can be referred to as filtered multi-tone multiple access system (FMT-MA). However, if the prototype filters are rectangular windows of duration NT, the system collapses to a discrete multi-tone multiple access system (DMT-MA).

2.3. Digital Implementation of the FMT Modulator

An efficient digital implementation of the transmitter is obtained by sampling at the Nyquist frequency, $1/T$, the signal (2), and assuming the prototype filters identical across carriers, i.e.,

$$X^u(nT) = \sum_{l=-\infty}^{\infty} g_1^u(nT-lNT)\sum_{k=0}^{N-1} x^{u,k}(lNT)e^{j\frac{2\pi}{N}kn} \tag{3}$$

According to (3) the FMT modulator is implemented by applying an IDFT on a block of N data symbols. Each IDFT output is filtered at rate $1/(NT)$ with the polyphase filters $g_{1,m}^u(lNT) = g_1^u(mT-lNT)$. Finally, after P/S conversion, D/A conversion and RF modulation follow.

If the filters are rectangular windows of duration NT, the filtering operation does not take place. Which is the well-known implementation of DMT modulation.

3. Asynchronous Channel Model

We assume that the users' signals propagate through independent frequency selective fading channels. Further, the signals are asynchronous, that is, they may have a time misalignment, and a frequency offset.

At the receiver side, we first run RF down conversion and low pass filtering with a broad band filter with nominal bandwidth W.

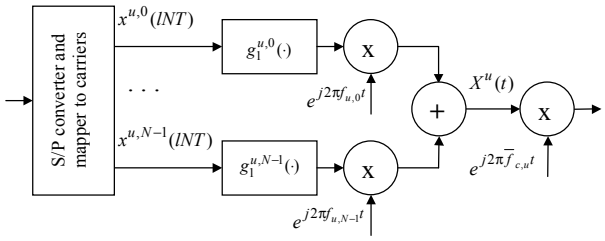

Fig. 1 . Multicarrier transmitter of user u.

Let $g_E^u(t)$ be the equivalent low pass impulse response of the cascade of the channel and the broad band front-end filter. Then, at the receiver side the composite low pass signal can be written as

$$y(t) = \sum_{u=1}^{N_U} e^{j2\pi\Delta f_u t} y^u(t-\Delta t_u) + \eta(t) \tag{4}$$

with

$$y^u(t) = \int_{-\infty}^{\infty} X^u(\tau)g_E^u(t-\tau)d\tau = \sum_{k=0}^{N-1}\sum_{l=-\infty}^{\infty} x^{u,k}(lNT)g_R^{u,k}(t-lNT) \tag{5}$$

and

$$g_R^{u,k}(t) = \int_{-\infty}^{\infty} e^{j2\pi f_{u,k}\tau} g_1^{u,k}(\tau)g_E^u(t-\tau)d\tau \tag{6}$$

being the overall impulse response of the *k-th* carrier (*k-th* sub-channel).

In (4) $\eta(t)$ is the thermal noise contribution that is assumed to be a white Gaussian process with zero mean and spectral density $2N_0$. The frequency offset between the RF carrier of user u and the local oscillator at the receiver is $\Delta f_u = \bar{f}_{c,u} - \bar{f}_c$. This may differ from zero because of the oscillator drifts and/or the movement of the users, and it is assumed small compared to W. The time offsets Δt_u are due to different transmission starting epochs and/or different propagation delays of users at different distance from the receiver.

4. Receiver Front-End Model

To perform detection, $y(t)$ is frequency offset compensated, and filtered with a bank of matched filters. These filters are matched to the sub-channel impulse responses that are defined in (6). Therefore, we have a bank of $\sum_{u=1}^{N_U} K_u$ filters that constitutes the receiver front-end. The matched filter outputs are sampled at rate $1/(NT)$ and are further processed to perform detection.

Optimal as well as sub-optimal detection algorithms are studied in [7]. In this paper we consider single user/carrier detection where decisions on the transmitted symbols are

[1] In (2) carrier spacing of $1/(NT)$ is implied.

made on a sub-carrier basis. Therefore, it is important to quantify the interference components between sub-channel matched filters outputs.

The matched filter output of user $\bar{u}$ and carrier $\bar{k}$ at time $\bar{l}NT$ is

$$z^{\bar{u},\bar{k}}(\bar{l}NT)=\int_{-\infty}^{\infty} y(t)e^{-j2\pi\Delta f_{\bar{u}}t}g_R^{\bar{u},\bar{k}*}(t-\bar{l}NT-\Delta t_{\bar{u}})dt \quad (7)$$

If we expand (7) we can write

$$z^{\bar{u},\bar{k}}(\bar{l}NT)=\sum_{u=1}^{N_U}\sum_{k=0}^{N-1}\sum_{l=-\infty}^{\infty} x^{u,k}(lNT)s^{u,\bar{u},k,\bar{k}}(l,\bar{l})+n(t) \quad (8)$$

with *n(t)* filtered thermal noise, and

$$s^{u,\bar{u},k,\bar{k}}(l,\bar{l})=\int_{-\infty}^{\infty} e^{j2\pi(\Delta f_u-\Delta f_{\bar{u}})t}g_R^{u,k}(t-lNT-\Delta t_u)g_R^{\bar{u},\bar{k}*}(t-\bar{l}NT-\Delta t_{\bar{u}})dt \quad (9)$$

being the cross correlation between two sub-channel impulse responses. Therefore,

$$z^{\bar{u},\bar{k}}(\bar{l}NT)=V_0x^{\bar{u},\bar{k}}(\bar{l}NT)+ISI+ICI+MAI+n(t) \quad (10)$$

Thus, the matched filter output sample corresponds to the transmitted symbol weighted by $V_0=s^{\bar{u},\bar{u},\bar{k},\bar{k}}(\bar{l},\bar{l})$, plus noise, and inter-symbol, inter-carrier, and multiple access interference components. The ISI is zero if and only if $s^{\bar{u},\bar{u},k,\bar{k}}(l,\bar{l})=0$, for all $l\neq\bar{l}$, and k, $\bar{k}$ assigned to user $\bar{u}$. The ICI is zero if and only if $s^{\bar{u},\bar{u},k,\bar{k}}(l,l)=0$, for all $k\neq\bar{k}$. The MAI is zero if and only if $s^{u,\bar{u},k,\bar{k}}(l,\bar{l})=0$.

The sub-channel cross correlations (9) depend upon the shape of the prototype filters, the channel impulse response, the time/frequency offsets, and the tone allocation strategy.

It is clear that single carrier detection based on observing (10) yields reliable decisions if the interfering components are low. In the next section we evaluate (9) for several filter shapes.

5. Evaluation of the Interference Components

In this section we quantify the interference levels at the sub-channel matched filter outputs when deploying prototype filters that are time limited, time limited with guard time, frequency limited, and Gaussian shaped.

In what follows it is convenient to define the following quantities.

$$\tau=(\bar{l}NT+\Delta t_{\bar{u}})-(lNT+\Delta t_u) \quad (11)$$

$$\nu=(f_{\bar{u},\bar{k}}+\Delta f_{\bar{u}})-(f_{u,k}+\Delta f_u) \quad (12)$$

Further the carriers are spaced, unless otherwise stated, by $1/(NT)$, i.e.,

$$f_{u,k}=k/(NT) \quad (13)$$

for *k=0,...,N-1*.

5.1. Time Limited Prototype Filters

Let the carriers be spaced according to (13), and let the prototype filters[2] be

$$g_1^{u,k}=\frac{1}{\sqrt{NT}}rect\left(\frac{t-NT/2}{NT}\right) \quad (14)$$

Further, let us assume the channel to be ideal, i.e., $g_E^u(t)=\delta(t)$. With these assumptions, we can calculate (9).

If $|\tau|<NT$ (15)

$$s^{u,\bar{u},k,\bar{k}}(l,\bar{l})=e^{j2\pi(\Delta f_u-\Delta f_{\bar{u}})(\bar{l}NT+\Delta t_{\bar{u}})}e^{j2\pi f_{u,k}\tau}e^{-j\pi\nu(NT-\tau)}\ldots$$
$$\ldots\frac{NT-|\tau|}{NT}sinc\left(\nu(NT-|\tau|)\right)$$

Otherwise, if $|\tau|\geq NT$, $s^{u,\bar{u},k,\bar{k}}(l,\bar{l})=0$.

Therefore, multiple access ISI and ICI arise because of time misaligned users. The ISI on a given carrier spans only the previous and the next symbol. Further, multiple access ICI is generated when the users are frequency misaligned.

When the channel is frequency selective both self and multiple access ISI and ICI are generated.

5.2. Rectangular Prototype Filters with Cyclic Prefix

Typically, a cyclic prefix is inserted when deploying DMT modulation. This allows for a simplified equalizer in inter-symbol interference channels. We here investigate the effect of using a cyclic prefix in the asynchronous DMT-MA scenario.

The insertion of such a cyclic prefix corresponds to transmit (*N*-μ) parallel data streams. Each has rate *1/*(*NT*), is filtered with,

$$g_T^{u,k}(t)=\frac{1}{\sqrt{NT}}e^{j2\pi f_{u,k}t}rect\left(\frac{t-(N-2\mu)T/2}{NT}\right) \quad (16)$$

where the carrier is $f_{u,k}=k/(NT-\mu T)$.

Efficient digital implementation is obtained by using a IDFT with (*N*-μ) points, and adding a prefix that is equal to the last μ IDFT outputs. Simple demodulation is accomplished by using a bank of N_U single user detectors. Each detector acquires time and frequency synchronization with the desired user. Then, it disregards the samples corresponding to the cyclic prefix. Finally, it runs a DFT with (*N*-μ) points. Each DFT output is sent to a decision device.

The operations deployed by the $\bar{u}-th$ detector correspond to partially match filter $y(t)e^{-j2\pi\Delta f_{\bar{u}}t}$ with

$$g_{part}^{\bar{u},\bar{k}}(t)=\frac{\sqrt{NT}}{(N-\mu)T}e^{j2\pi f_{\bar{u},\bar{k}}t}rect\left(\frac{t-(N-2\mu)T/2}{(N-\mu)T}\right) \quad (17)$$

Assuming an ideal channel impulse response, it follows that the matched filter output exhibits cross-terms,

---

[2] $rect(\frac{t}{T})=\begin{cases}1 & |t|\leq T/2\\ 0 & |t|>T/2\end{cases}$, $sinc(t)=\sin(\pi t)/\pi t$.

$$s^{u,\bar{u},k,\bar{k}}(l,\bar{l}) = e^{j2\pi(\Delta f_u - \Delta f_{\bar{u}})(\bar{l}NT+\Delta t_{\bar{u}})} e^{j2\pi f_{u,k}\tau} e^{-j\pi\nu T(N-2\mu)} \cdots \quad (18)$$
$$\cdots \; sinc\left(\nu T(N-\mu)\right)$$

for $|\tau| \le \mu T/2$. If no frequency offsets are present among distinct users, (18) is zero. Therefore, the insertion of a cyclic prefix longer than the maximum time misalignment allows for reduced interference levels.

Other results on DMT-MA can be found in [3]-[5].

5.3. Frequency Limited Prototype Filters

Let us consider an FMT-MA system with carrier spacing according to (13), and frequency limited prototype filters that are defined as follows

$$g_1^{u,k} = \frac{1}{NT} sinc\left(\frac{t}{NT}\right) \quad (19)$$

If we assume an ideal channel impulse response, the computation of (9) yields the following results.

If $|\nu| < 1/(NT)$ (20)

$$s^{u,\bar{u},k,\bar{k}}(l,\bar{l}) = e^{j2\pi(\Delta f_u - \Delta f_{\bar{u}})(\bar{l}NT+\Delta t_{\bar{u}})} e^{j2\pi f_{u,k}\tau} e^{j\pi\tau\nu} \cdots$$
$$\cdots \left(\frac{1}{NT} - |\nu|\right) sinc\left(\tau\left(\frac{1}{NT} - |\nu|\right)\right)$$

Else if $|\nu| \ge 1/(NT)$, $s^{u,\bar{u},k,\bar{k}}(l,\bar{l}) = 0$.

From these results we can conclude saying that the FMT-MA system in the presence of an ideal channel exhibits multiple access ICI due to frequency misaligned users. The ICI contribution on a given carrier is due only to the left-right adjacent carriers. Further, multiple access ISI is present on a given carrier only if the same carrier is assigned to other time misaligned users.

If the channel is frequency selective and introduces resolvable echoes, then any user does not experience any self ICI, however each of its carriers exhibits self ISI.

Some excess bandwidth will always be present in practical systems. A possible practical choice is to use squared root raised cosine filters or Gaussian shaped filters. In the next section we investigate the latter choice.

5.4. Gaussian Prototype Filters

In this section we consider the deployment of Gaussian shaped filters. From a practical standpoint, they can be considered time and frequency limited provided that an appropriate cut off frequency f_{3dB} is used,

$$g_1^{u,k}(t) = \sqrt{\frac{\alpha}{\sqrt{\pi/2}NT}}\, e^{-(\frac{\alpha}{NT}t)^2} \quad (21)$$

with $\alpha = \pi f_{3dB} NT\sqrt{2/\ln 2}$. Assuming an ideal channel and carrier spacing according to (13), the computation of (9) yields,

$$s^{u,\bar{u},k,\bar{k}}(l,\bar{l}) = e^{j\pi(f_{u,k}+f_{\bar{u},\bar{k}})\tau} e^{j\pi(-\Delta f_u + \Delta f_{\bar{u}})(\tau+2lNT+2\Delta t_u)} \cdots$$
$$e^{-(\frac{\alpha}{\sqrt{2}NT}\tau)^2} \; e^{-(\frac{\pi NT}{\sqrt{2}\alpha}\nu)^2} \quad (22)$$

From (22) it can be seen that the ICI, ISI, MAI components can be controlled by an appropriate choice of f_{3dB}.

6. FMT-MA System Design Guidelines

From the analysis above, we have shown that in a FMT-MA system self ICI, self ISI, and MAI components are present at the outputs of the matched filter bank. These components are a function of the prototype filter shape, the tone allocation strategy, the amount of time/frequency offset among users, and the channel conditions. Low interference levels require filters that are limited in time and in frequency, with carriers that are allocated as far as possible among users. In particular:

1. With time limited filters, a frequency selective channel is responsible for ICI, ISI, and MAI. Time offsets and frequency offsets among users yield a MAI contribution. The ISI contribution on a given carrier spans only the previous and the next symbol.
2. With time limited filters and cyclic prefix, it is possible to counteract the time misalignments across users as well as the echoes from a frequency selective channel.
3. With frequency limited filters it is possible to counteract the ICI from time misalignments and channel echoes. However, the frequency offsets yield ICI contributions. Further, ISI is always present.
4. With filters that are practically limited in time and in frequency it is possible to reduce the ICI, ISI, and MAI. For instance, Gaussian filters are a reasonable choice.
5. Lower MAI is generated when the tones are allocated to users in disjoint blocks. With the block allocation of tones we can insert frequency guards in order to further separate the spectrum of distinct users.

It should also be noted that some degree of time and frequency synchronization might be obtained in some applications. For instance, a method based on a control loop from the base station is described in [8].

In order to quantify the interference components we plot in Fig. 2-6 the magnitude of (9), $|s^{u,\bar{u},k,\bar{k}}(l,\bar{l})|$, as a function of carrier spacing when the two carriers experience a given time misalignment and/or a given frequency offset. In the figures $f_1 - f_2 = (\bar{k}-k)/(NT)$, $\bar{l} = l_1$, $l = l_2 = \{\bar{l}-1, \bar{l}, \bar{l}+1\}$.

Further, we fix the bandwidth and we consider the deployment of N=16 and N=64 carriers. Therefore, if we fix the value of time offset (8T in the figures), and frequency offset (0.125/16/T in the figures) we see that by increasing the number of carriers we can diminish the interference level from the time misalignment, but we increase the one due to the frequency offset.

In particular in Fig. 2-3 we use rectangular filters. In the presence of only frequency offsets no ISI arises. However, in the presence of time offsets both ISI and ICI appear.

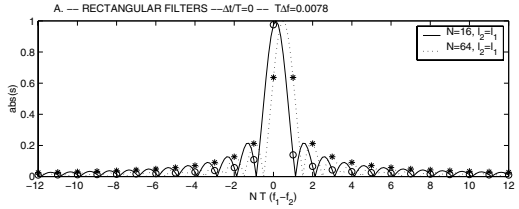

Fig. 2. Magnitude of cross correlation (9) as a function of carrier spacing. Rectangular filters with both N=16 and N=64 carriers. No time misalignment, and frequency offset Δf=0.0078/T.

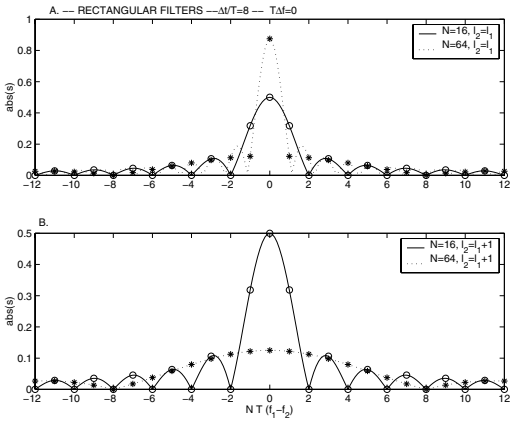

Fig. 3 . Magnitude of cross correlation (9) as a function of carrier spacing. Rectangular filters with both N=16 and N=64 carriers. Time misalignment Δt=8T, and no frequency offset.

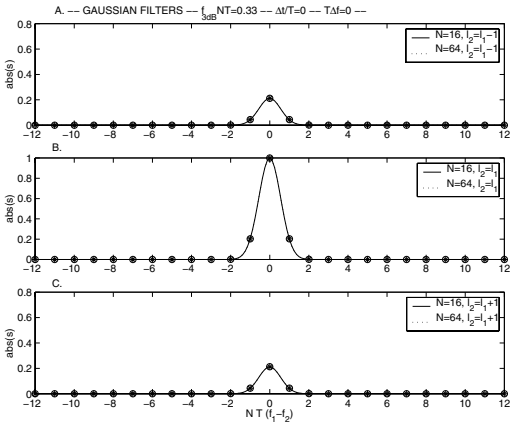

Fig. 4 . Magnitude of cross correlation (9) as a function of carrier spacing. Gaussian filters with f_{3dB}NT=0.33, and both N=16 and N=64 carriers. No time misalignment, and no frequency offset.

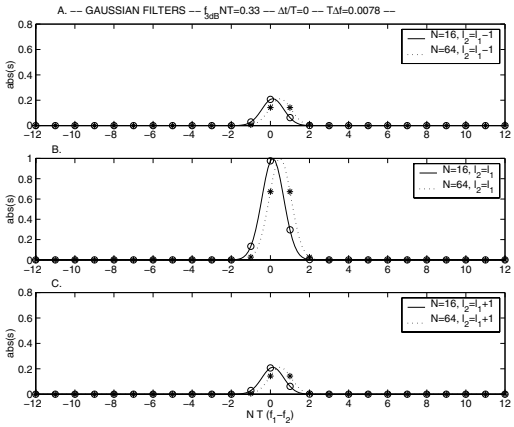

Fig. 5. Magnitude of cross correlation (9) as a function of carrier spacing. Gaussian filters with f_{3dB}NT=0.33, and both N=16 and N=64 carriers. No time misalignment, and frequency offset Δf=0.0078/T.

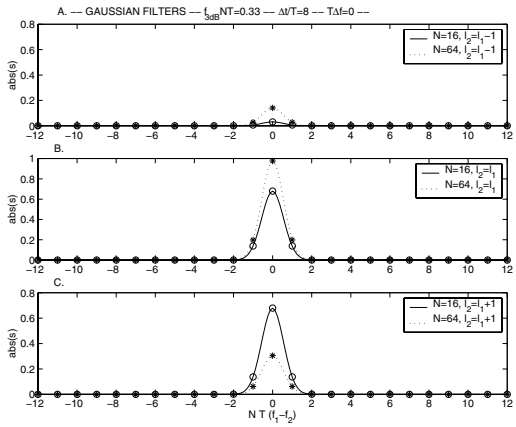

Fig. 6 . Magnitude of cross correlation (9) as a function of carrier spacing. Gaussian filters with f_{3dB}NT=0.33, and both N=16 and N=64 carriers. Time misalignment Δt=8T, and no frequency offset.

In Fig. 4-6, we consider Gaussian shaped filters with f_{3dB}NT=0.33. Note that in the absence of both time and frequency offset a certain amount of ICI and ISI is always present. However, diminishing f_{3dB} can reduce the ICI at the expense of the ISI. Note that in Fig. 4, the ISI essentially spans two adjacent symbols, and the ICI two adjacent carriers. Further the N=16 and N=64 curves overlap.

Fig. 5 shows that in the presence of a frequency offset the ICI increases. In the presence of a time offset the ICI is not altered with respect to Fig. 4 but the ISI increases.

7. Performance Results

In this section we report performance results from simulations. We consider a two users system with N=16 carriers. Each user is assigned with 8 distinct carriers. The allocation is either block or interleaved. We compare both DMT and FMT options. In the latter case the filters are Gaussian with f_{3dB}NT=0.33. The modulation format is 4-PSK.

The users transmit their signals through an AWGN channel with a time offset that is uniformly distributed in [-8T, 8T] and with a frequency offset that is uniformly distributed in [-0.125/(NT), 0.125/(NT)].

Single carrier detection is deployed, that is, we make decisions on the symbols/bits transmitted on a given carrier from the observation of the corresponding sub-channel matched filter output (10). Other optimal and sub-optimal detection approaches are studied in [7].

Fig. 7 shows average bit-error rate versus signal-to-noise ratio. We also plot the performance of 4-PSK in AWGN which is the performance lower bound (from [9]). Note that all curves exhibit an error-rate floor. However, DMT with block allocation can significantly lower such a floor.

Improved performance can be achieved through multi-user detection and interference cancellation methods, as proposed in [7]. As well we can deploy channel coding. Fig. 8 shows bit-error rate performance when deploying a rate 1/2 convolutional code with memory 2 and 4-PSK modulation. Still single carrier detection is used. The performance is greatly improved and exceeds the uncoded bound in all cases with the exception of DMT with interleaved tones.

These performance results show that when single carrier detection is deployed DMT with block allocation is a better

option. However, when more sophisticated detection approaches are used, FMT can allow for reduced complexity detection algorithms. Further, lower MAI is induced with the block allocation strategy, which translates into better performance. However, the interleaved allocation may yield better diversity gains in frequency selective fading channels.

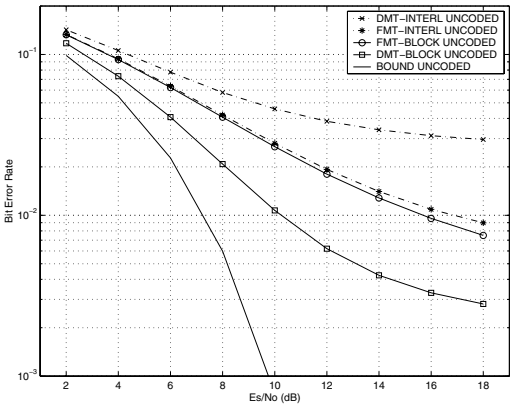

Fig. 7 . Average bit-error-rate versus SNR in AWGN with 2 Users, 8 carriers/users, rectangular (DMT) and Gaussian (FMT) filters. Uncoded 4-PSK modulation. Users have a uniformly distributed time offset in [-8T, 8T] and a uniformly distributed frequency offset in [-0.125/(NT), 0.125/(NT)].

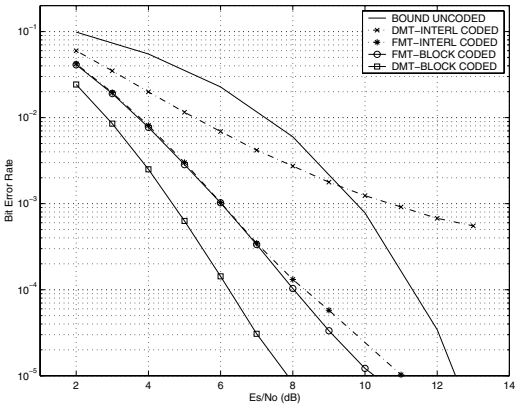

Fig. 8 . Average bit-error-rate versus SNR in AWGN with 2 Users, 8 carriers/users, rectangular (DMT) and Gaussian (FMT) filters. Coded 4-PSK modulation with a rate 1/2 convolutional code with memory 2. Users have a uniformly distributed time offset in [-8T, 8T] and a uniformly distributed frequency offset in [-0.125/(NT), 0.125/(NT)].

8. Conclusions

We have investigated the use of FMT and DMT architectures for multi-user asynchronous communications. We have shown through analysis that ISI, ICI, and MAI components arise at the output of the sub-channel matched filters at the receiver. The interference components are a function of the transmit filters, the tones allocation, the channel characteristics, and the amount of time/frequency offsets across the users. In particular, closed expressions for the interference have been calculated when deploying time limited filters, frequency limited filters, and Gaussian filters.

As a result, we have found that in a DMT multi-user system we can allocate blocks of contiguous tones to distinct users, and add appropriate time and frequency guard intervals. In this case, the MAI due to time offsets and multi-path fading can be completely removed, while the MAI due to the frequency offset can be significantly lowered.

In a multi-user FMT system the prototype filters have to be designed with the general objective of generating low self inter-carrier and inter-symbol interference. Further, the tone allocation strategy can contribute to yielding low MAI. The deployment of Gaussian shaped filters turns out to be a good choice.

Finally, we have reported results from simulations showing that convolutionally coded DMT-MA with allocation of tones to users in disjoint blocks can achieve reliable performance with a simple detection approach.

9. References

[1] G. Cherubini, E. Eleftheriou, S. Olcer, J.M. Cioffi, "Filter bank modulation techniques for very high-speed digital subscriber lines", *IEEE Communications Magazine*, May 2000, pp. 98-104.

[2] S. Kaiser, W. Krzymien, "Performance effects of the uplink asynchronism is a spread spectrum multi-carrier multiple access system", *European Trans. on Telecomm.*, July-August 1999, pp. 399-406.

[3] A. Tonello, N. Laurenti, S. Pupolin "Analysis of the uplink of an asynchronous DMT OFDMA system impaired by time offsets, frequency offsets, and multi-path fading", *Proceedings of IEEE Vehicular Technology Conference 2000 Fall*, Boston, USA, September 24-28, 2000, pp. 1094-1099.

[4] A. Tonello, N. Laurenti, S. Pupolin, "Capacity considerations on the uplink of a DMT OFDMA system impaired by time misalignments and frequency offsets", *Proc. of 12th Tyrrhenian Workshop on Digital Comm.*, Isola D'Elba, Italy, September 13-16, 2000.

[5] A. Tonello, N. Laurenti, S. Pupolin, "On the effect of time and frequency offsets in the uplink of an asynchronous multi-user DMT OFDMA system", *Proc. of International Conference on Telecommunications 2000*, Acapulco, Mexico, May 22-25, 2000, pp. 614-618.

[6] L. Cimini Jr. "Analysis and simulation of a digital mobile channel using orthogonal frequency division multiplexing", *IEEE Trans. on Comm.*, July 1985, pp. 665-675.

[7] A. Tonello "Optimal and sub-optimal detection/decoding in asynchronous multiple access OFDM communication systems", *to be submitted to IEEE Trans. on Communications*, 2001.

[8] J. van de Beek, P. O. Borjesson, et al. "A time and frequency synchronization scheme for multiuser OFDM", *IEEE JSAC*, November 1999, pp. 1900-1914.

[9] J. G. Proakis, " Digital Communications", *McGraw-Hill*, 1995.